

A STUDY OF THE EFFECTS OF BLADE SHAPE ON ROTOR NOISE

Henry E. Jones
U.S. Army Joint Research Program Office/AFDD
Casey L. Burley
NASA Langley Research Center

Abstract

A new rotor noise prediction system called the Tiltrotor Aeroacoustic Code (TRAC) has been developed under the Short Haul (Civil Tiltrotor) program between NASA, the Army, and the U.S. helicopter industry. This system couples the comprehensive rotorcraft code CAMRAD.Mod1 with either the high resolution sectional loads code HIRES or the full potential CFD code FPRBVI to predict unsteady blade loads, which are then input to the noise prediction program WOPWOP. In this paper, HIRES will be used to predict the blade-vortex interaction (BVI) noise trends associated with blade shape. The baseline shape selected was a 17% scale model of a contemporary design 4 bladed rotor. Measurements for this rotor were acquired in the Duits-Nederslandse Windtunnel (DNW). The code is used to predict noise for the base configuration and the results are compared to the measured data. This provides a firm foundation for investigating the BVI noise trends associated with blade shape. The shapes selected for study are based on variation of sweep and taper which reflect plausible "passive" design concepts. Comparisons of power required, integrated noise, and aerodynamics are made and important trends are noted.

Nomenclature

a_0	freestream sound speed, m/sec
V	freestream velocity, m/sec
b	number of blades
c	blade mean chord, m
R	rotor radius, m/sec
ρ	air density, kg/m ³
Ω	rotational speed, rpm
σ	blade solidity ratio, $bc/\pi R$
μ	rotor advance ratio, $V/\Omega R$

c rotor aerodynamic reference blade chord
 c_{tip} rotor blade chord at tip

C_T rotor thrust coefficient, $\frac{T}{\rho\pi(\Omega R)^2 R^2}$

r spanwise coordinate along blade

DNW Duits-Nederslandse Windtunnel

FW-H Ffowcs Williams-Hawkings equation

Y_{BAR} spanwise location of vorticity, measured from tip

BPF rotor blade passage frequency; 96.17 Hz

BVISPL sound pressure level obtained by integrating from the 7th through 30th harmonics of the BPF (nominally 673 Hz to 2885 Hz), dB

λ blade sweep angle, deg

β' observer elevation angle, deg

Ψ' observer azimuthal angle, deg

p_{max} pressure variable in WOPWOP model

N force, newtons

m meters

Background

Impulsive rotor noise is caused by rapid changes in the local aerodynamic environment of the blade. Until recently, computing these effects has been beyond the state of the art, and hence experimental studies were used to investigate the relevant phenomena. Brooks¹ provides an excellent review of much of this work. Recently, a new rotor noise prediction system called the Tiltrotor Aeroacoustic Code (TRAC) has been developed under the Short Haul (Civil Tiltrotor) program between NASA, the Army, and the U.S. helicopter industry. The code system has, to date, been successfully demonstrated on a model tiltrotor configuration by Burley²; furthermore, subsets of the system have also been presented by Brooks³, Visintainer⁴, and Brentner⁵. The current effort continues the exploration of the application of this new system. Here, for the first time, the system as a whole is

Presented at the AHS Technical Specialists' Meeting for Rotorcraft Acoustics and Aerodynamics; Williamsburg, VA, October 28-30 1997

used to explore conventional rotors within the context of a geometric parameter sweep. The goal is to test the ability of TRAC, with all of its modeling assumptions, to predict noise trends for a family of rotors. A complete study of all the issues associated with the solution of this problem would be beyond the scope of this paper, hence we will restrict the discussion to wake modeling, rotor loads, and blade-vortex interaction (BVI) noise. The emphasis will be on the use of TRAC and the predicted results and not on the relative merits of a particular design.

The paper is divided into three sections: an introduction to the system of codes, application of the method to a single configuration and a brief correlation with experimental data, and the blade geometry study.

The Tiltrotor Acoustics Code System: TRAC

TRAC consists of a set of computational tools which, taken together, provide a prediction method for the complex multi-disciplinary problem of rotor acoustics. Figure 1 depicts the flow of data between the various codes within the system. For the current effort, the CAMRAD.Mod1-HIRES-WOPWOP method is employed.

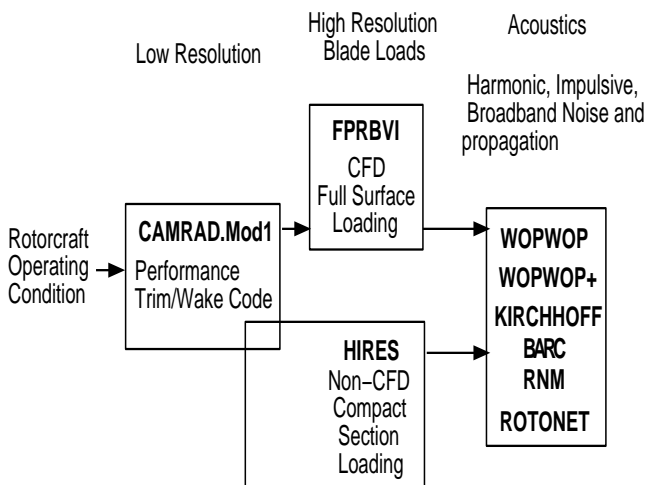


FIGURE 1. TRAC flowchart.

Rotorcraft Trim

The CAMRAD.Mod1 computer code is capable of predicting the dynamics, aerodynamics, loads, and performance of a trimmed rotorcraft system in a wind tunnel or in flight. The basic method makes use of lifting line theory coupled with airfoil section force and moment data tables to compute the load on the blade. The method is described in some detail by Brooks.³ Basically, CAMRAD.Mod1 is a highly modified version of the original CAMRAD⁶ model. The

essential methodology of the original model is retained; however, a number of key enhancements and modifications have been made, including increased azimuthal resolution, swept planform effects, indicial aerodynamic blade response modeling, and vortex roll-up modeling. The resulting method is much more suited to the prediction of noise.

Computational results from CAMRAD.Mod1 provide the spanwise blade section loading, performance, and trim solution for the rotor. Additional processing is required to produce the high resolution solution of the rotor wake, blade motion, and sectional loading solution which is necessary for noise prediction.

Compact Section Loading

HIRES is an extension to the CAMRAD.Mod1 which is executed following the trim calculation. HIRES is typically used to compute blade loads at .5 degrees azimuthal step and at 100 radial stations. These high temporal and spanwise resolution loads are obtained by recomputing the wake velocity influence coefficients for recalculated blade motion and interpolated wake geometries at each azimuth step. The aerodynamic calculations in HIRES are accomplished in a post-processing program which uses the high-resolution definition of the induced velocity over the rotor disc. The resulting high resolution lift and drag are then available for use with the acoustic prediction code.

Acoustics

After the TRAC modules have produced the high resolution airloads, the acoustics propagation model WOPWOP^{7,8} is employed to predict the noise level at specified microphone locations. WOPWOP is the coding of acoustic formulation 1A of Farassat⁷, which is a time domain solution to the FW-H equation, excluding the volume source or “quadrupole” term. It was developed as a method to predict the discrete frequency noise of helicopter rotors, and is valid for arbitrary blade motion, geometry, and observer location. The HIRES option of TRAC provides high-resolution section blade loads which are converted into equivalent “compact” pressures acting at a specified chord location (usually the local quarter chord).

Test Data

A limited correlation with test data will be conducted in order to provide a firm foundation for the planform study. The data will be compared to acoustic data from the 1989 aeroacoustic test conducted in the DNW.⁹ The test was part of the U.S. Army Aerodynamic and Acoustic Testing of Model

Rotors (AATMR) Program and involved U.S. Government agencies and United Technologies Corporation (UTC).

Application of the Method

In this section, a set of results for a base configuration will be used to establish formats, to introduce the use of the system, and for a limited correlation. Predictions will fall into three categories: (1) wake geometry; (2) rotor airloads, and (3) rotor acoustics.

The CAMRAD.Mod1 model provides the user with a rich choice of options for use in predicting rotor performance, loads, and acoustics. These models include extensive treatments of the rotor structural and aerodynamic environments. Before proceeding, it is, therefore, important to establish the modeling options to be used. This will provide a frame of reference within which comparisons can be made. The following assumptions are employed for the study:

1. an isolated main rotor in a wind tunnel
 - a. $R = 1.428$ m
 - b. $a_0 = 338.19$ m/sec
 - c. $\rho = 1.226$ kg/m³
 - d. $\Omega = 1442.5$ rev/min
 - e. $V_{TIP} = 215.7$ m/sec
 - f. $\lambda = 20^0$ (at $r=.94$ for base configuration)
2. shaft axes at 5.15^0 (modeling descent)
3. $C_T/\sigma = 0.0714$
4. $\mu = .151$
5. constant blade area for each configuration
6. linear blade twist of -12^0 (except for baseline)
8. The full free-wake model (3 iterations) with multiple vortex trailers and a multi-core (9) vortex model
9. The blade structural response will be modeled with six bending modes and 1 torsion mode.

Rotor Wake

Performance and wake data are presented to support the acoustic results. Of particular interest here is the vortex roll-up behavior. Figure 2 is a plot of the predicted tip and secondary vortex spanwise emission locations as a function of azimuth. Note the presence of the secondary vortex which is deposited into the wake beginning at 30^0 azimuth and existing until about 190^0 . Also note the sharp decrease in Y_{bar} at 80^0

and 150^0 , in contrast to the smoother changes which occur on the retreating side of the disc. The secondary vortex features much more rapid variations in Y_{bar} and is not present on the retreating side. It will later be shown that the primary BVI for this configuration occurs near the azimuth angle of about 75^0 , just before the sharp change in Y_{bar} for both vortices. The source of the vortex is at about $\Psi = 120^0$. Another interesting issue related to the rotor wake is the loading distribution during the actual BVI which is presented in figure 3. Note especially, the multiple loading peaks for this condition, most probably a result of predicted multiple interactions. It should be noted that the actual BVI was not measured or observed during the test but measured blade loads indicate similar trends.

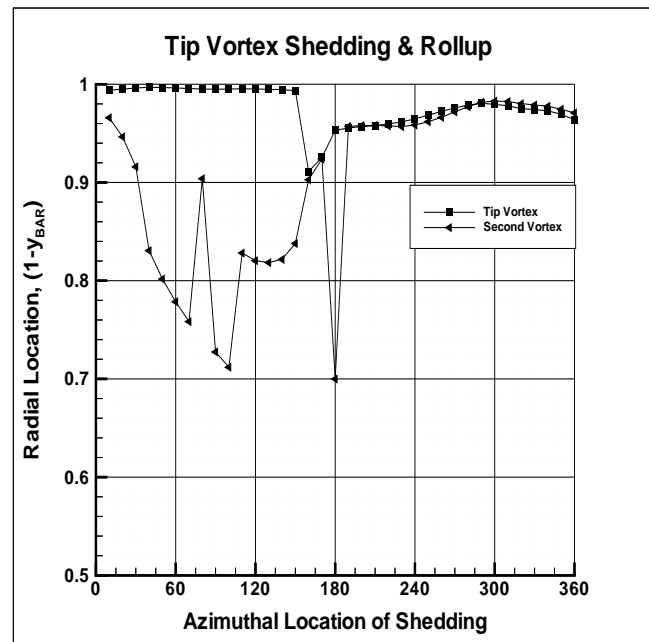


FIGURE 2. Predicted spanwise emission locations for both the tip and secondary vortices

Rotor Airloads

Rotor airloads will be presented as contours of loading (in N/m) over the rotor disc of the blade as in figure 4 below. Of particular interest in this figure are the regions of dense “bands” which indicate high temporal gradients. When these bands are near parallel to the rotating blade, BVI impulsive noise results. It is seen that this occurs in the first quadrant between azimuth angles of 60^0 and 90^0 and on the retreating side between about 290^0 and 310^0 .

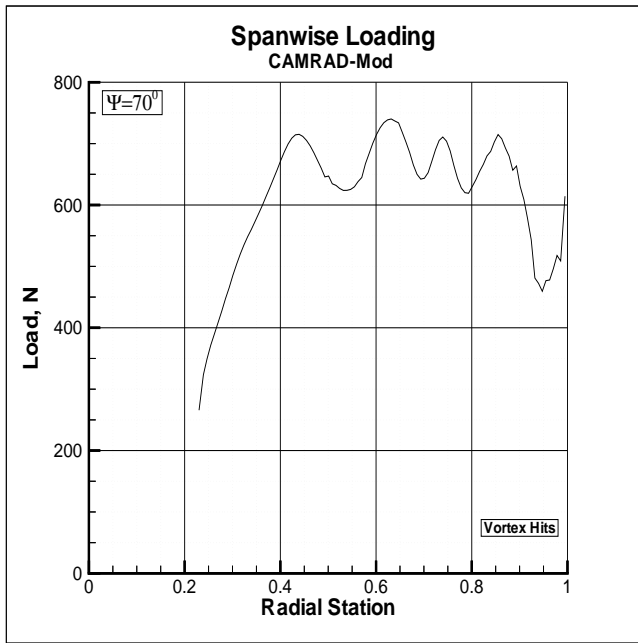


FIGURE 3. Spanwise blade load during vortex encounter, Baseline configuration (HIRES)

Baseline Blade
Shaft Angle = 5.15
CT/S = .0714

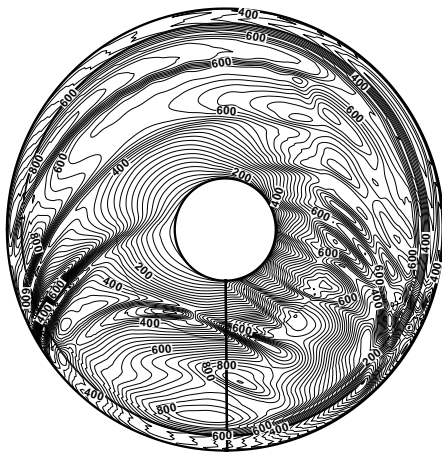


FIGURE 4. Contour of blade loading for base configuration. (HIRES)

Rotor Acoustics

Acoustic Signal

As stated above, the WOPWOP code predicts the noise time histories and sound pressure level (SPL) generated by the blade at a user specified microphone location. In the WOPWOP code, the loading must be given as a force distribution over the blade surface. Since CAMRAD.Mod1/HIRES computes sectional

loads, the input WOPWOP subroutines were adapted to utilize such a loading description.

In WOPWOP the pressure on the lower surface is assumed to be zero and the upper surface pressure is given by:

$$p = \begin{cases} 0 & (x/c) < .2 \\ 20((x/c) - .2)p_{max} & .2 < (x/c) < .25 \\ 20((x/c) - .3)p_{max} & (x/c) > .3 \end{cases}$$

where p_{max} is set such that the total section lift is the same as that produced by the distributed load. The WOPWOP blade motion is specified using the predicted results from CAMRAD.MOD1. The first and second harmonics of rigid blade flap, lead-lag and 1st torsion are considered.

Figure 5 compares the measured and predicted noise time history at a microphone location 25° below the advancing side. The figure shows that the TRAC system is capable of computing the BVI noise amplitude including important blade passage features and BVI events, but that many of the details, such as blade to blade variations of the waveform are still beyond the ability of the system to capture.

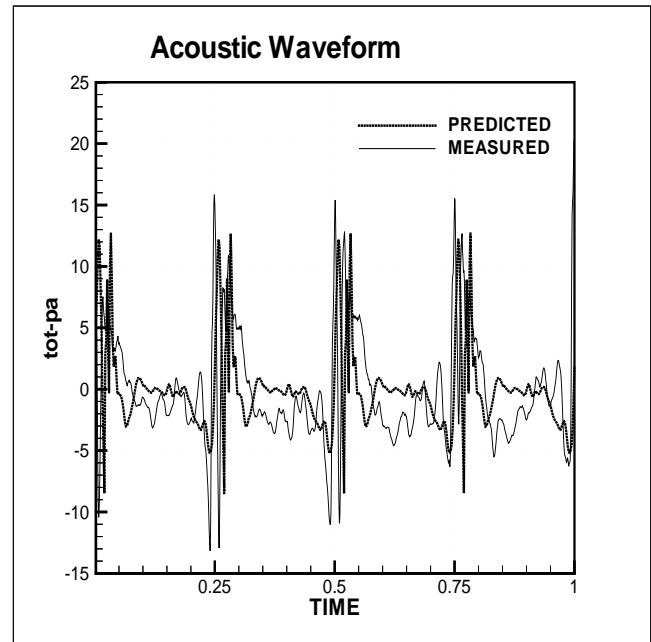


FIGURE 5. Sound pressure level for base configuration at a specified microphone location compared with test data. (HIRES)

Noise Directivity

It has long been recognized that the impulsive loading of the BVI generates a highly directional acoustic field. It follows that a large number of

observer locations must be computed to capture this effect. To study this characteristic, Brentner⁵ proposed that the sound be predicted on a sphere of 1.5 rotor diameters centered on the rotor hub. The observer locations lie at 15° increments on the sphere surface in the region $-60^{\circ} < \Psi' < 60^{\circ}$ and $30^{\circ} < \beta' < -210^{\circ}$, where Ψ' and β' are the azimuth and elevation angles shown in figure 6.

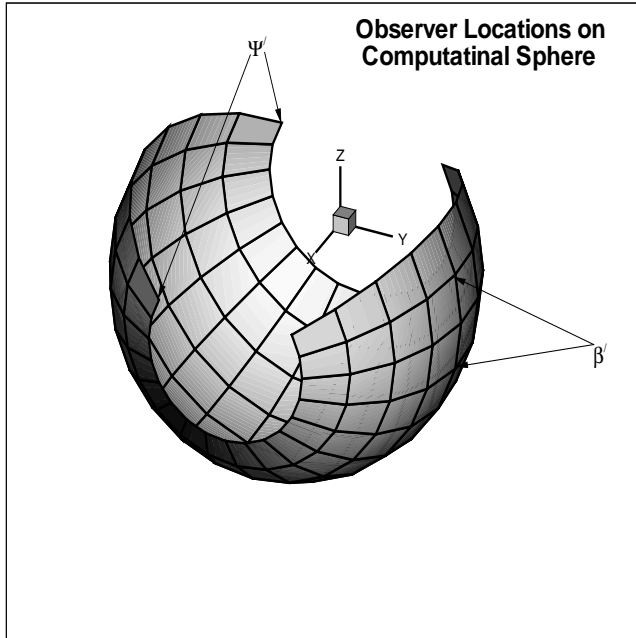


FIGURE 6. Geometric distribution of observers in a “bowl” around the rotor.

The noise predictions are presented as contours of the midrange noise metric which is the sum of the 7th through 30th harmonic of the blade passage frequency of the overall sound pressure level (OASPL) on the Ψ - β plane. Figure 7 gives this result for the baseline rotor.

The figure shows two regions of focused high noise: a large region centered around $(\Psi, \beta) = (20^{\circ}, -60^{\circ})$ at about 101 dB.; and a smaller but more intense region centered at $(\Psi, \beta) = (-45^{\circ}, -150^{\circ})$ at about 105 dB. Both these regions can be related to the high loading gradients seen in figure 4.

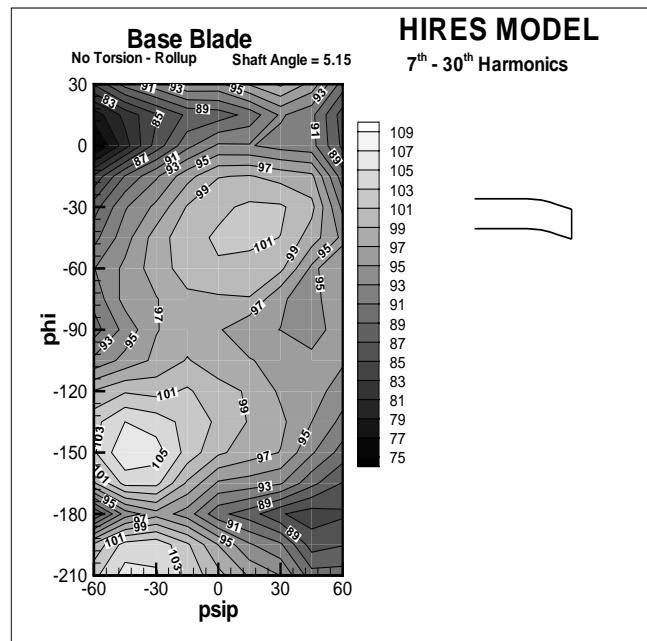


FIGURE 7. Directivity pattern for predicted mid-range noise of baseline blade. (HIRES)

Blade Planform Study

The remainder of the paper will deal with the blade planform study. The shapes selected for study are based on variation of sweep and taper which reflect plausible “passive” designs of a family of conventional single main rotor configurations. Figure 8 provides a tabular and visual summary of the configurations. Each configuration is assumed to have the same mass and stiffness distributions. Furthermore, airfoil section shape and distribution are held constant as is the sweep angle of 20° . Chord and sweep location are the only variables. Chord is changed via a tapering of the blade and by moving the location of the taper initiation point. The sweep initiation point is also varied. For each of the configurations, the root chord has been modified in order to maintain a constant blade area. Twist is held constant at -12° , except for the baseline which has a highly non-linear twist distribution. Finally, a five bladed version of the last swept-tapered configuration is examined. The configurations can be viewed as being “grouped” with the LinTwt, Lamda1, and Lamda2 group representing taper changes, and LamdaSwp1, LamdaSwp2, and LamdaSwp3 representing sweep changes. The Base and LinTwt configurations show the effect of twist and the LamdaSwp3 and Blds configurations show the effect of number of blades.

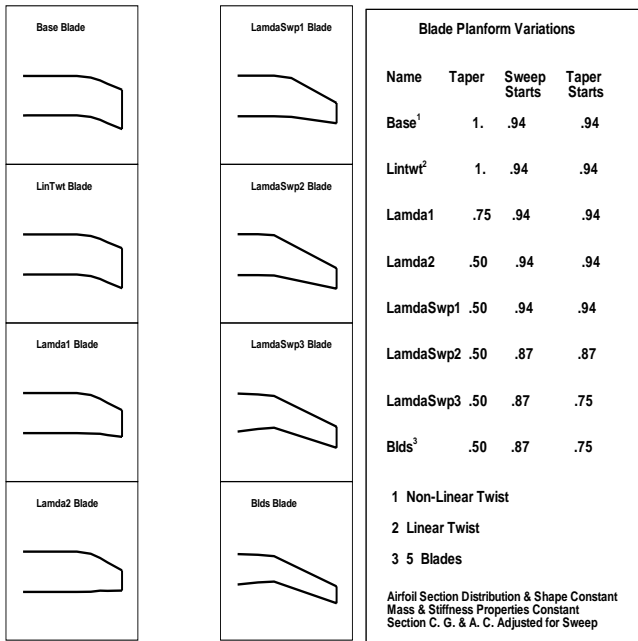


FIGURE 8. Planform views of blade shapes.

Rotor Performance and Wake

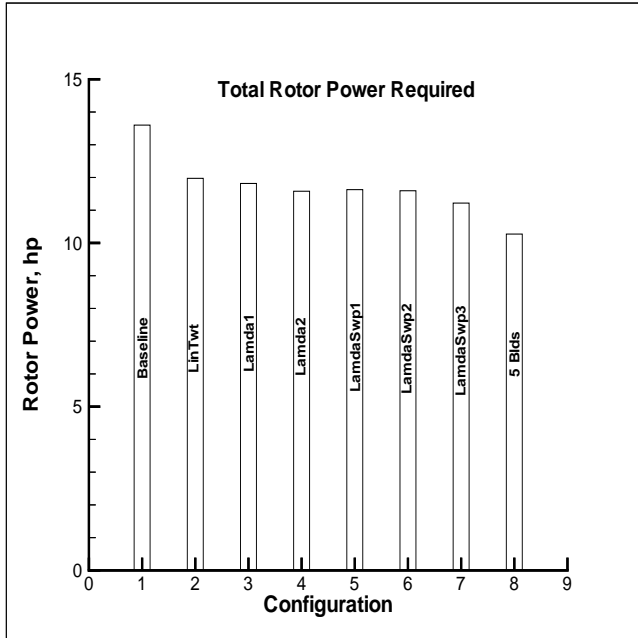


FIGURE 9. Rotor power required at test point.

Figure 9 is a summary chart of the predicted rotor power required for the test condition. The figure shows a clear trend in power with shape/geometry change. HIREs is executed following the trim computation, and it is from its results that the details necessary to predict the rotor BVI phenomena are obtained.

Rotor BVI effects are influenced by four wake related factors: blade loading at the time the vortex is generated, blade loading during the BVI, wake geom-

etry (miss distance), and vortex strength during the interaction. The issue here is how the blade loading changes with shape, and how this affects the vortex rollup. Table 1 gives a summary of the key (closest) BVI events for each blade. The major interaction for most of the configurations is in the first quadrant between 65 and 75 degrees azimuth; the first swept-tapered blade is an unexplained exception. Another feature of these interactions is that it would seem that each blade has at least several encounters at the same location. The source of these vortices all seem to be located in the second quadrant at about 120⁰ azimuth.

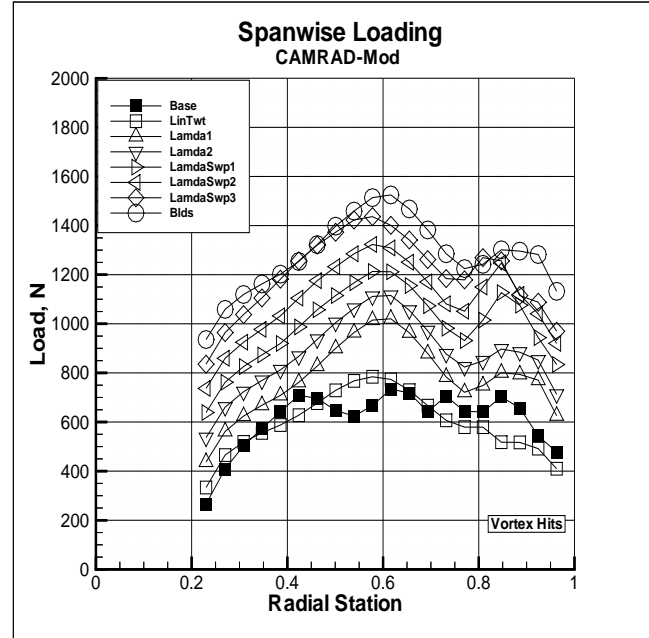


FIGURE 10. Blade radial loading at the major BVI location for each configuration; HIREs model.

Figure 10 presents the spanwise blade loading for each configuration at the location of the principal BVI. Please note that the “zero” for each configuration is shifted by 200 N in order to separate the curves for easy viewing. With the exception of the baseline rotor, which has exceptionally large variations (or response), the remaining blades show a similar loading curve, with the geometric changes appearing as variations in the location of the peaks. Note that a general trend of shifting load inboard follows the location of the taper/sweep initiation point. Also note the small variation at the location of sweep initiation.

Figure 11 gives the vortex centroid locations, that is the final rolled-up position, for the various configurations. Note that except for the baseline configuration, the vortex rollup follows a smooth pattern. The roll-up behavior seems to “group” with geometry, that is, LinTwt-Lamda1-Lamda2 all have similar

behavior as does the LamdaSwp1-LamdaSwp2-LamdaSwp3 group.

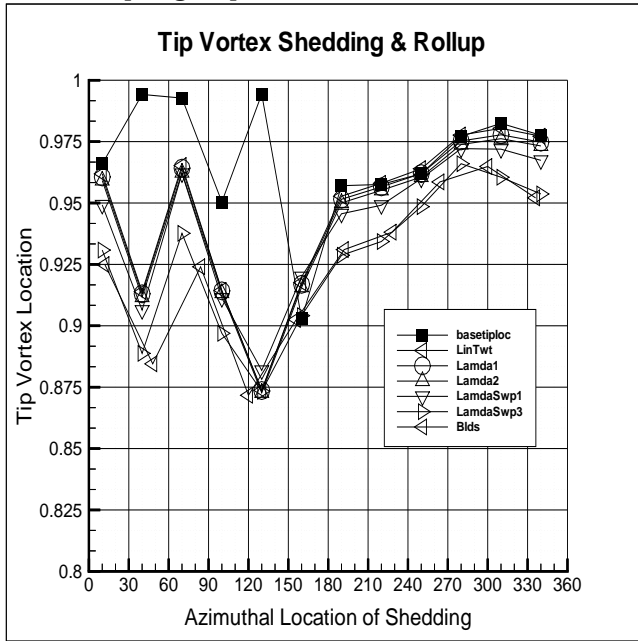


FIGURE 11. Tip vortex roll-up characteristics.

Airloads

Airload contour plots for representative configurations are presented in figures 12-17.

Figures 12, and 13 present the effect of twist change on the loading: note here, the increase in loading gradient in the second quadrant. The spanwise extent of a BVI is more apparent for the linear twist configuration. An increase in the noise as a result of the increased lateral coherence is expected and shown in the next section. Figures 13 and 14 show the effect of taper: the changes here are mostly in details with no major impact. Figures 14 and 15 show the effect of sweep change: here there is a noticeable reduction in loading gradient especially in the first quadrant. Figures 16 and 17 show the change with blade number. There is a definite reduction in the intensity of the gradients on the disc.

Baseline Blade
Shaft Angle = 5.15
CT/S = .0714

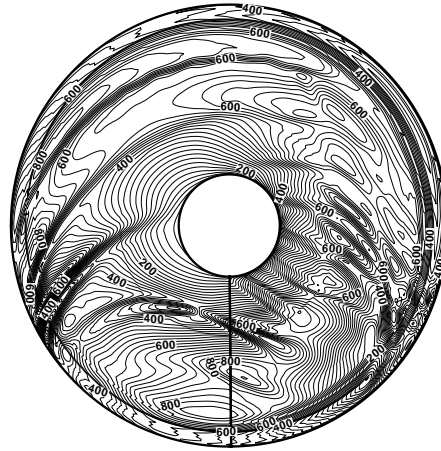


FIGURE 12. Contour of blade loading for base configuration. (HIRES)

LinTwt Blade
Shaft Angle = 5.15
CT/S = .0714

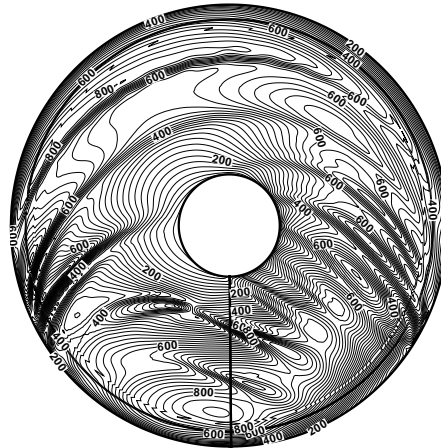


FIGURE 13. Contour of blade loading for linear twist configuration. (HIRES)

Lamda2 Blade
Shaft Angle = 5.15
CT/S = .0714



FIGURE 14. Contour of blade loading for second tapered configuration. (HIRES)

LamdaSwp3 Blade
Shaft Angle = 5.15
CT/S = .0714

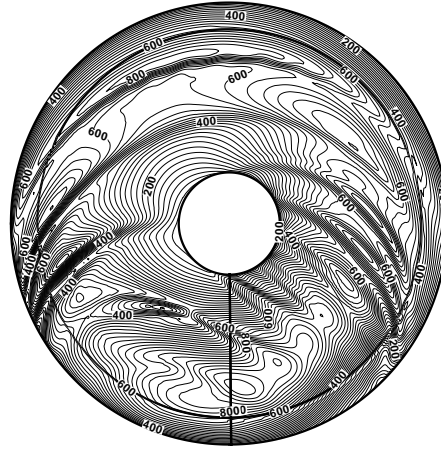


FIGURE 16. Contour of blade loading for third swept-tapered configuration. (HIRES)

LamdaSwp1 Blade
Shaft Angle = 5.15
CT/S = .0714

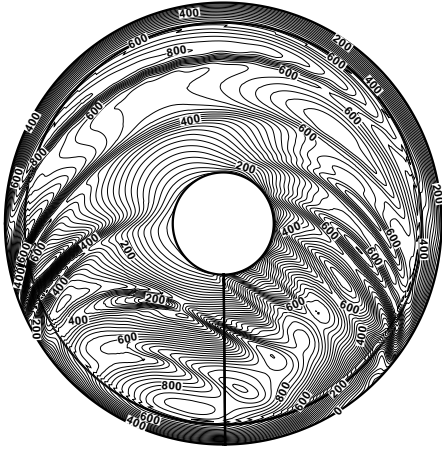


FIGURE 15. Contour of blade loading for first swept-tapered configuration. (HIRES)

Blds Blade
Shaft Angle = 5.15
CT/S = .0714

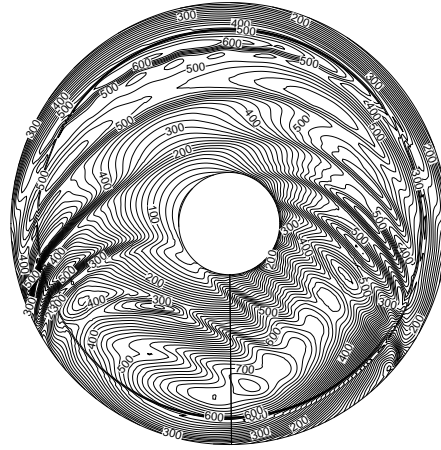


FIGURE 17. Contour of blade loading for five bladed configuration. (HIRES)

Acoustic Predictions

Signal Characteristics

The loading predictions are utilized to predict the noise for the various configurations. Figures 18-21 give the comparison of the noise signal at a single microphone location (corresponding to the “hot” spot noted in figure 10) for the key geometric changes.

Figure 18 shows the effect of changing twist from linear to non-linear; note here the shift in phase and the reduction in some of the peak pressures. Figure 19 gives the effect of taper, which appears to have little or no effect. Figure 20 gives the effect of sweep location, which appears to be mostly a phase change. Finally, figure 21 gives the effect of number of blades; shown here is the obvious change in peak location due to the shift in blade-passage frequency, but also a general reduction in the amplitude.

Noise Directivity

Noise directivity contour results are shown in figures 22 to 29. The acoustic results using the HIREs blade loading show a noise ‘hot’ spot on both the advancing and retreating sides, with the most intense region on the retreating side. The blade loading contours (figures 12-17) for these conditions, indicate high loading levels and strong gradients on the retreating side. The wake geometry results predict a single strong tip vortex, with a small miss distance for this region, whereas on the advancing side there is typically two vortices of lesser intensity. In general the advancing side ‘hot’ spot consistently was at a level of 101 dB for all the blade configurations, except for the 5-bladed rotor, where the level decreased significantly by 5 dB. This is expected since the load is distributed among 5 blades rather than 4, and the resulting tip vortices should be weaker.

Several changes in the noise directivity and level as a function of twist and sweep are of note. The linear twist results compared to the baseline (and all others) shows a much larger advancing side ‘hot’ spot. The HIREs airloads produce a considerable reduction in the size of the advancing side ‘hot’ spot for a change in the sweep location.

Integrated Acoustics

Figure 30 gives the integrated noise result in bar chart format. Note here especially the drop in noise between the linear and non-linear configurations Base-LinTwt. Also note the sharp drop for the five-bladed configuration. The other configurations show a steady drop in noise with taper and sweep location which parallels the trend seen in power.

Figure 31 gives the change in noise with shaft angle. Here, the “noise slope” for each configuration is seen to “group” with geometry - the LinTwt-Lamda1-Lamda2 all have slopes of about 3dB/deg while the LamdaSwp1-LamdaSwp2-LamdaSwp3 are at about 2.8~2.9dB/deg. The Base slope is ~2dB/deg while the five-bladed configuration is ~2.2dB/deg. These differences may be due to the strength of the vortex encountered. Note from table 1 that LinTwt-Lamda1-Lamda2 all have “hits” from the tip (i.e. stronger) vortex, whereas all others have at least one hit from a secondary vortex.

Figure 32 is taken from reference 1 and represents the only source of data which can be used to assess the validity of figure 31. These data were taken for a variety of blades and are operating at different conditions. Also the data-base was sparse. In spite of this, the general comparison between these figures, qualitatively shows similar trends.

Comments and Observations

Rotor noise prediction is a complex problem. In order to meet this challenge, the TRAC system has evolved from a number of different disciplines (dynamics, aerodynamics, and acoustics) into an integrated tool.

The following observations can be made:

1. TRAC is capable of predicting the basic noise level of a conventional rotor even with geometrically complex features such as non-linear twist and sweep.
2. Noise can be affected using “passive” blade designs.
3. Noise effects seem to “group” within Architectures (i.e. shape, twist, or number of blades).
4. Architectural changes, especially step changes, have a greater effect on noise than do parametric changes (i.e. taper).
5. The trends predicted for overall noise as a function of shaft angle are similar to those obtained from experimental studies.

Issues which remain for future study include:

1. Addition of a surface loading model to the CAMRAD.Mod1 system.
2. Improved wake modeling within CAMRAD.Mod1,
3. Continued investigation using the FPRBVI CFD post processor.

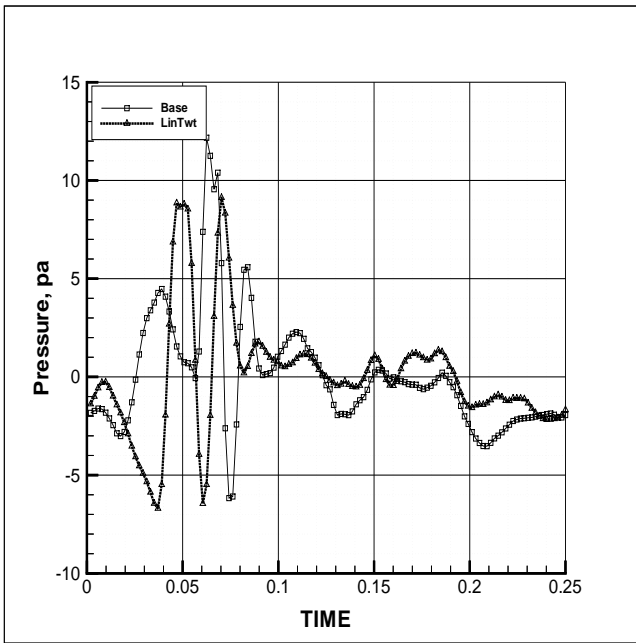


FIGURE 18. Effects of non-linear twist on noise signal.

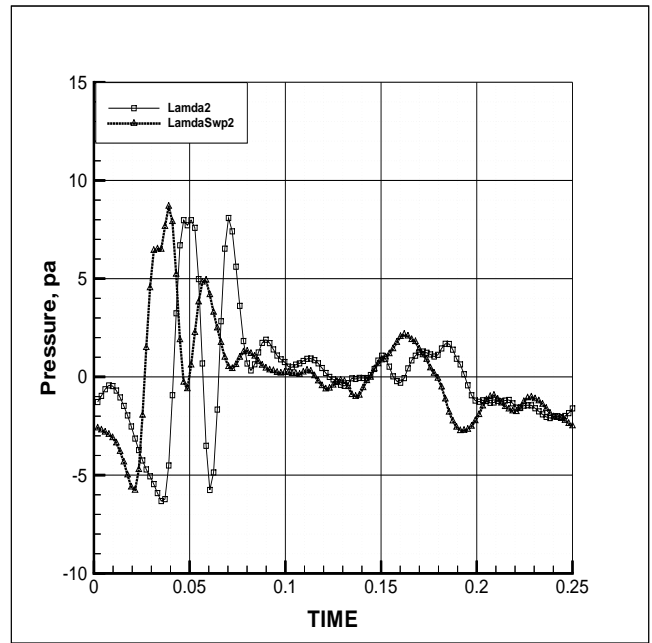


FIGURE 20. Effects of sweep location on noise signal.

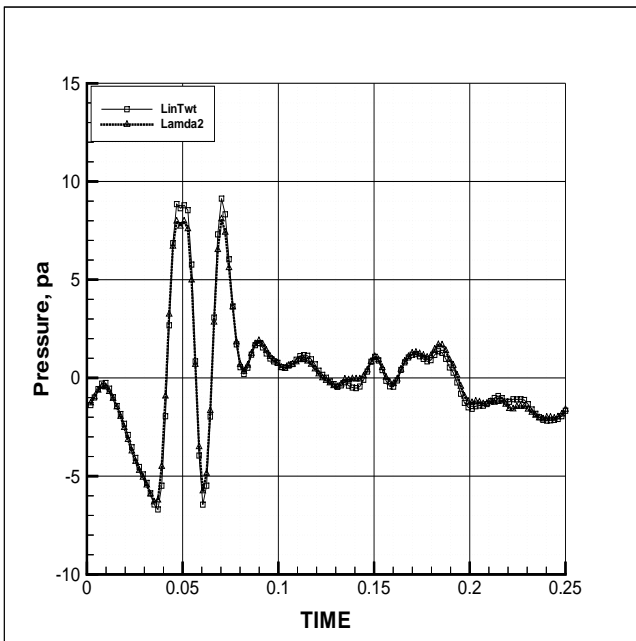


FIGURE 19. Effects of taper on noise signal.

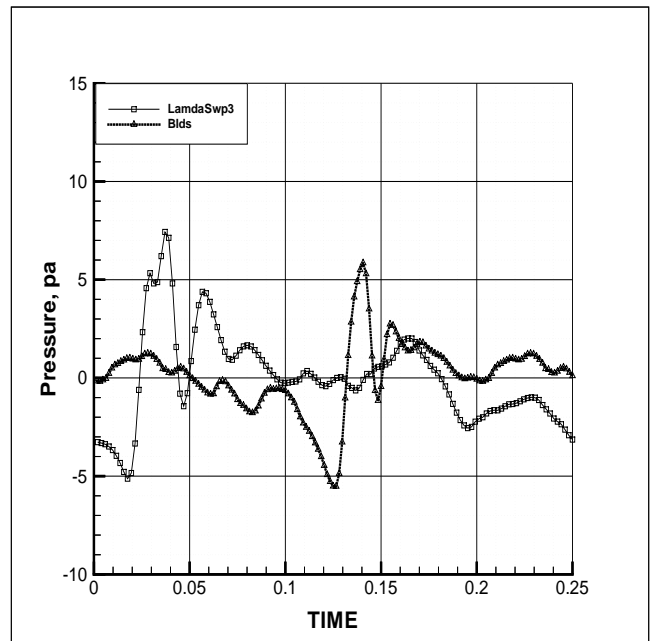


FIGURE 21. Effects of blade number on noise signal

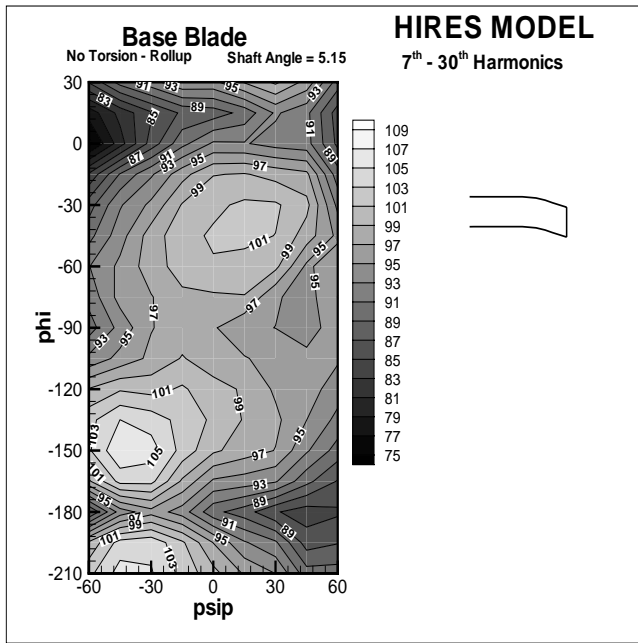


FIGURE 22. Directivity pattern for predicted mid-range noise of baseline blade. (HIRES)

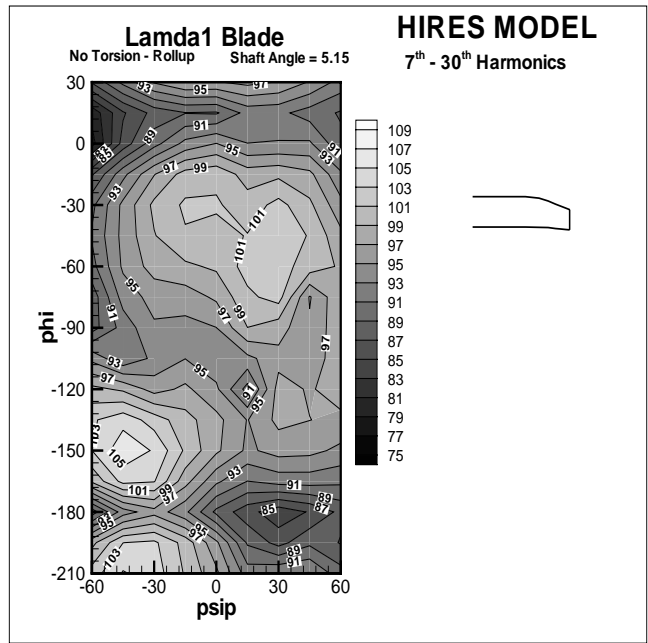


FIGURE 24. Directivity pattern for predicted mid-range noise of first tapered blade.

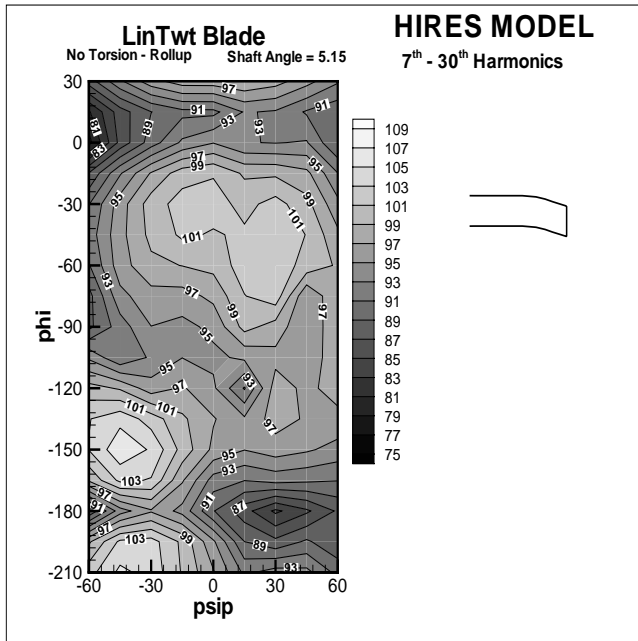


FIGURE 23. Directivity pattern for predicted mid-range noise of linear twist blade.

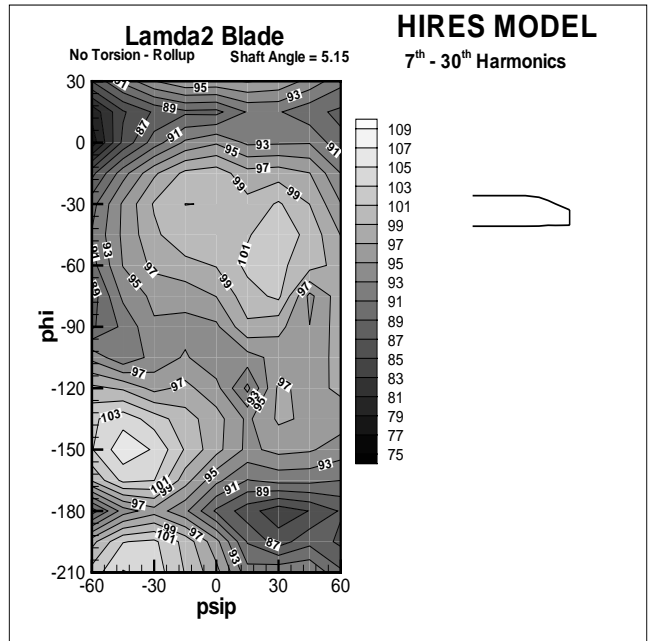


FIGURE 25. Directivity pattern for predicted mid-range noise of second tapered blade.

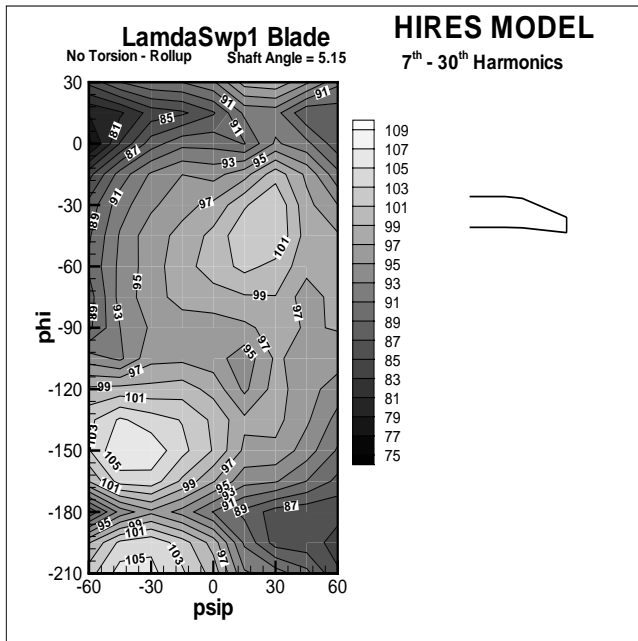


FIGURE 26. Directivity pattern for predicted mid-range noise of first swept-tapered blade.

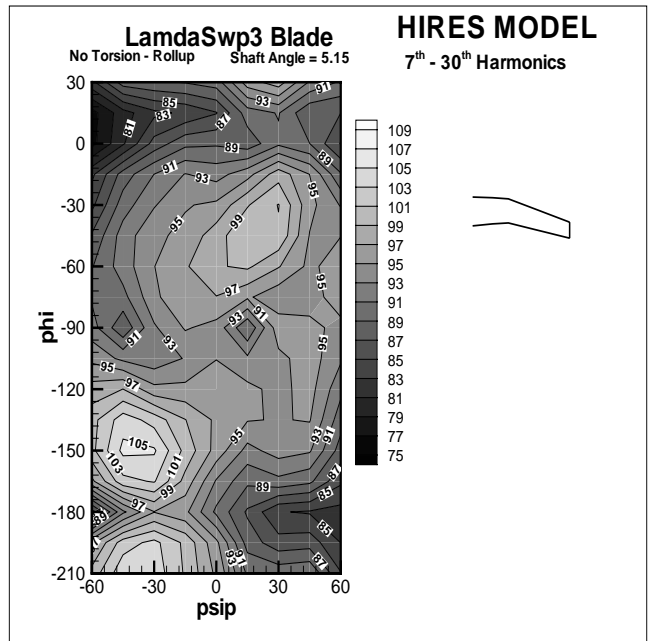


FIGURE 28. Directivity pattern for predicted mid-range noise of third swept-tapered blade.

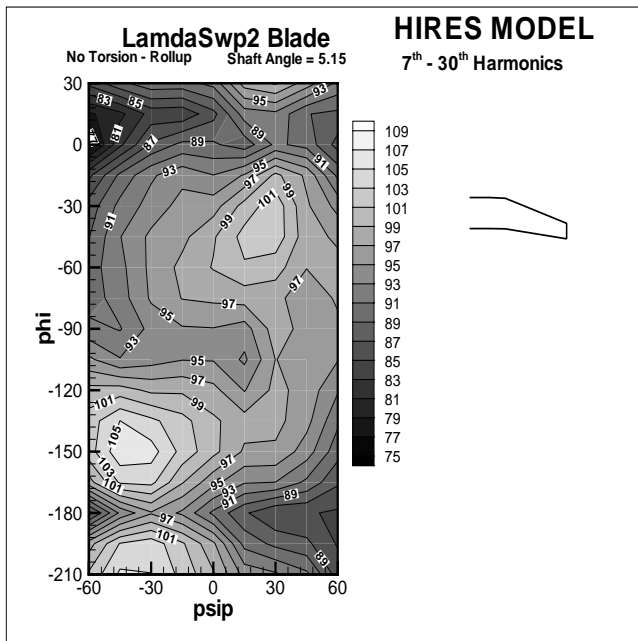


FIGURE 27. Directivity pattern for predicted mid-range noise of second swept-tapered blade.

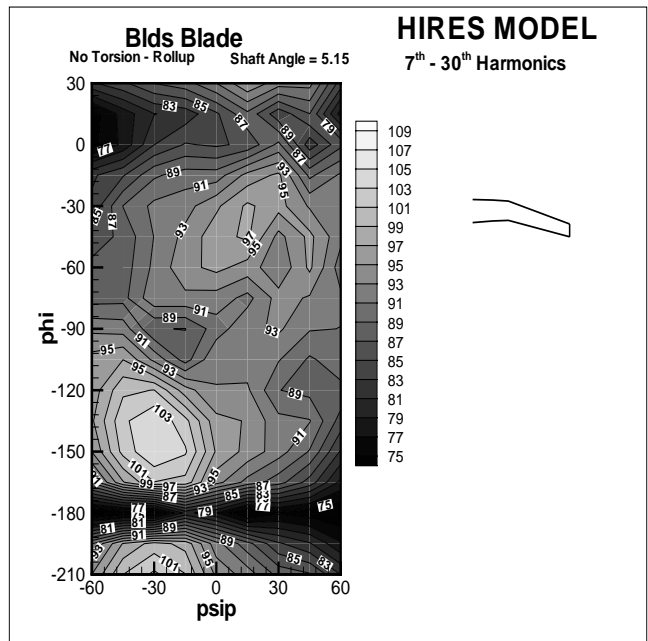


FIGURE 29. Directivity pattern for predicted mid-range noise of five-bladed rotor.

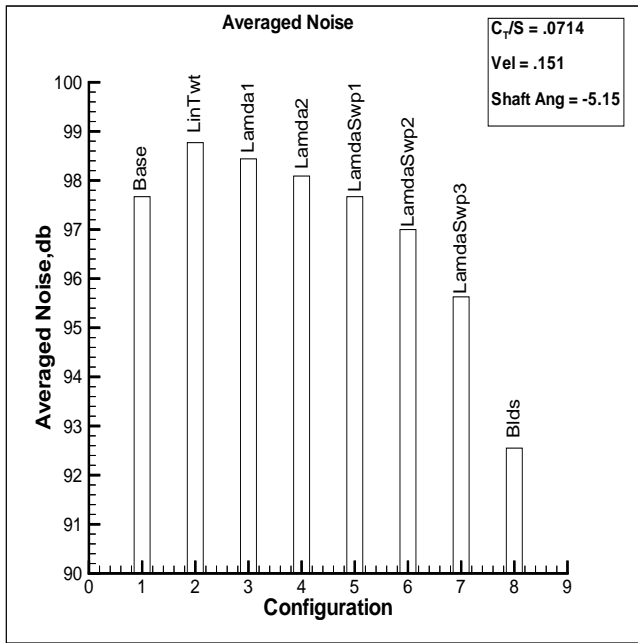


FIGURE 30. Averaged BVISPL for each configuration.

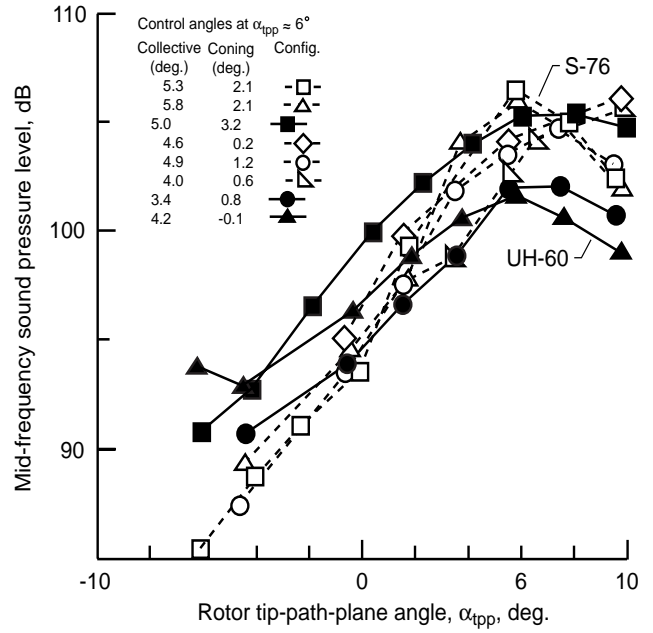


FIGURE 32. Variation of averaged noise with shaft angle (test data) (ref 1)

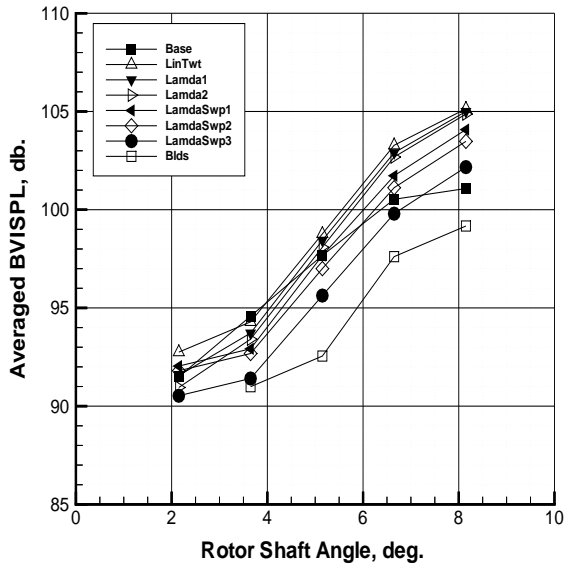


FIGURE 31. Variation of averaged noise with shaft angle (prediction)

References

1. Brooks, Thomas F.: Studies of Blade-Vortex Interaction Noise Reduction by Rotor Blade Modification. NOISE-CON 93. May 1993
2. Burley, Casey L.; Marcolini, Michael A.; Brooks, Thomas F.; Brand, Albert G.; and Conner, David A.: Tiltrotor Aeroacoustic Code (TRAC) Predictions and Comparison with Measurements. AHS 52nd Annual Forum, Washington 1996.
3. Brooks, Thomas F.; Boyd, Douglas D.; Burley, Casey L.; Jolly, Ralph J.: Aeroacoustic Codes for Harmonic and BVI Noise-CAMARD.Mod1/HIRES. 2nd AIAA/CEAS Aeroacoustics Conference. May 1996
4. Visintainer, Joseph A.; Burley, Casey L.; Marcolini, Michael A.; and Liu, Sandy R.: Acoustic Predictions Using Measured Pressures from a Model Rotor in the DNW
5. Brentner, Kenneth S.; Marcolini, Michael A.; and Burley, Casey L.: Sensitivity of Acoustic Predictions to Variations of Input Parameters. AHS Technical Specialists Meeting on Rotorcraft Acoustics and Fluid Dynamics. October 1991
6. Johnson, Wayne: A Comprehensive Analytical Model of Rotorcraft Aerodynamics and Dynamics Parts I,II,&III. NASA TM 81182 1980.
7. Farassat, F.; and Succi, G.P.: The Prediction of Helicopter Rotor Discrete Frequency Noise. Vertica, vol 7, no. 4, 1983, pp309-320.
8. Brentner, Kenneth S.; Prediction of Helicopter Rotor Discrete Frequency Noise, *A Computer Program Incorporating Realistic Blade Motions and Advanced Acoustic Formulation*. NASA TM 87721 1986.
9. Yu, Y. H., Liu, S. R., Landgrebe, A. J., Lorber, P.F., Jordan, D. E., Pallack, M.J., and Martin, R.M.; "Aerodynamic and Acoustic Test of a United Technologies' Model Scale Rotor at DNW." AHS 46th Annual Forum, Washington DC, May 1990.

Table 1: BVI Interaction Locations And Sources

Blade	Miss Distance	Location of Interaction	Deposited at Azimuth	From Trailer*
Base	0.01R	75.0	140.	2
LinTwt	0.0125R	70.0	125.	1
Lamda1	0.0125R	70.0	125.	1
Lamada2	0.0125R	70.0	125.	1
LamdaSwp1	0.01R	310.0	200.	1,2
LamdaSwp2	0.01R	65.0	115.	2
LamdaSwp3	0.01R	65.0	115.	1,2
Blds	0.01R	66.0	114.	1

* Note: Trailer 1 from main tip vortex and Trailer 2 from inboard tip vortex